



SEISMIC DAMAGE ASSESSMENT IN ERZINCAN (TURKEY) UTILIZING SYNTHETIC GROUND MOTION RECORDS

S. Karimzadeh⁽¹⁾, A. Askan⁽²⁾, M. A. Erberik⁽³⁾, A. Yakut⁽³⁾

⁽¹⁾ Graduate Student, Civil Engineering Department, Middle East Technical University, Ankara

⁽²⁾ Assoc. Prof., Civil Engineering Department, Middle East Technical University, Ankara

⁽³⁾ Prof., Civil Engineering Department, Middle East Technical University, Ankara

Abstract

Loss estimation studies exercised for seismically active regions generally require fragility analyses to be performed which necessitate the use of ground motion records. These records could be 'real', i.e. recorded, acceleration time series or for regions with sparse ground motion data, 'synthetic' records consistent with the regional seismicity and produced using alternative simulation techniques. This study mainly concentrates on seismic damage estimation of Erzincan, which is a city on the eastern part of Turkey located in the conjunction of three active faults as right lateral North Anatolian Fault, left lateral North East Anatolian Fault and left lateral Ovacik fault, considering both regional seismicity and local building information. For this purpose, to generate a set of scenario earthquakes by using regional seismicity parameters of Erzincan, Stochastic Finite Fault Methodology has been followed as the simulation technique. Then, existing building stock are classified into specified groups that are represented with equivalent single-degree-of-freedom systems where the inelastic dynamic structural characteristics of the models are investigated. The response statistics of the structures are evaluated through non-linear time history analysis. Finally, the suitability of the methodology is evaluated by comparing the estimated damage levels with the observed ones during the 1992 Erzincan earthquake. The results seem to have a reasonable match in between.

Keywords: Erzincan, Regional Seismicity, Stochastic Finite-fault Method, Local Buildings, Seismic Damage



1. Introduction

Seismic risk estimation is of particular interest, especially in seismically active urban areas, in order to reduce structural and economic losses. Identification of seismic risk in any area is performed in two steps: The first step is assessment of potential seismic hazard in the region of interest by performing regional seismic hazard analyses, while the second step involves vulnerability analyses including structural fragility quantification and building damage assessment. This study focuses on seismic damage assessment based on simulated ground motion records and local building data.

Estimation of seismic damage is crucial for Turkey, which is one of the most seismically active countries in the world. For estimation of seismic damage and losses due to large near field events, it is important to consider the effects of earthquake rupture process. In regions with sparse ground motion data, ground motion simulations provide alternative regional time histories accounting for the specific features of the fault and the kinematics of the rupture process.

On the other hand, local building data is also necessary to estimate the building damage and consequent losses in a reliable manner. Majority of the building stock in different parts of Turkey consists of low-rise and mid-rise Reinforced-Concrete (RC) frame structures as well as unreinforced masonry buildings. Most of these structures have deficiencies and usually they are not designed according to seismic design codes to resist strong ground shaking. Therefore, it is critical to investigate the seismic risk by considering the regional building stock.

Until recently, majority of the past studies related to damage and loss estimation used generic information regarding either the building stock or ground motion records. However, there are few studies [e.g.: 1, 2] on development of seismic fragility curves using both regional building characteristics and seismicity of the area of interest.

In this study, as the study region, Erzincan, which is located in the Eastern Part of Turkey and in the close vicinity of the North Anatolian Fault Zone (NAFZ), is selected. Erzincan is a city with relatively sparse ground motion networks. For regions with limited recorded data, ground motion simulations provide synthetic time histories with different levels of magnitude. It is aimed herein to assess the seismic damage of a specified region by using both local structural parameters as well as regional synthetic ground motion records of the corresponding study area. To validate the proposed methodology, the estimated damage is compared with the observed damage during the 1992 Erzincan earthquake. Finally, the potential seismic damage for a scenario event in the region with $M_w=7$ is presented.

2. Study Area

North Anatolian Fault (NAFZ) is an active right-lateral strike-slip fault that lies in Northern Turkey and is one of the most active fault zones in the world. In the last century, NAFZ led to the most destructive events in Turkey such as the 1939 Erzincan ($M_s\sim 8.0$) event in the eastern part (Fig. 1) as well as the 1999 Kocaeli ($M_w=7.4$) and 1999 Düzce ($M_w=7.2$) earthquakes in the western part close to Istanbul.

Erzincan is one of the most hazardous cities in Eastern Turkey located in a tectonically complicated area, at the conjunction of three strike slip faults: the right lateral North Anatolian Fault, the left lateral North East Anatolian Fault, and the left lateral Ovacik fault. In addition to the 1939 event, Erzincan suffered from another destructive earthquake in 1992 ($M_w=6.6$) that led to significant structural damage as well as mortalities (Fig. 1).

According to the General Statistic Agency in Turkey (TÜİK), majority of the buildings in Erzincan (79%) are residential. Thus, the focus of this study is damage estimation of only residential buildings.

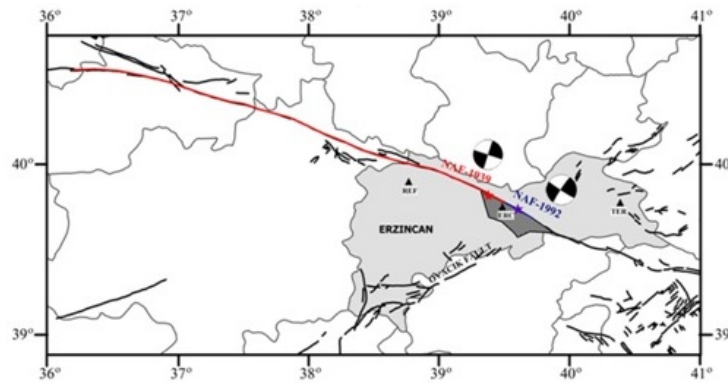


Fig. 1 – Seismotectonics in the Erzincan region with the fault systems and the epicenters of the 1939 and 1992 events (Adopted from [3]). The study region lies within the shaded area which is Erzincan basin and the city center

3. Strong Ground Motion Simulation

This part includes ground motion simulation methodology followed by its applications in the study area.

3.1 Methodology: Stochastic finite-fault technique

Estimation of reliable simulated time histories is the fundamental objective of all ground motion simulation techniques varying from deterministic to stochastic methods. Overall, ground motion simulation techniques can be divided into three main groups: deterministic, stochastic, and hybrid simulations. Deterministic approaches need details of seismic sources along with highly-resolved velocity models to accomplish the numerical solution of the seismic wave equation for full wave propagation purposes (e.g.: [4]). These methods are generally practical for relatively lower frequencies. Stochastic techniques combine the deterministic far field S-wave spectrum with random phases [5]. These techniques have intrinsic limitations due to absence of full wave propagation effects, still they are used efficiently worldwide for numerous seismic regions in the form of either point-source or finite-fault modeling (e.g.: [6, 7]). Hybrid methods combine deterministic and stochastic approaches for the simulation of low and high frequency components, respectively (e.g.: [8]).

In this study, since there exist no high-resolution velocity models of shallow soil layers for Erzincan region, deterministic models are out of scope. A recent form of stochastic finite-fault modeling by Motazedian and Atkinson [6] which was shown to provide realistic broadband frequencies for engineering purposes is used.

3.2 Simulations along Eastern segment of NAFZ

Erzincan is a city with relatively sparse ground motion networks. Therefore, in this section, it is aimed to perform ground motion simulations for scenario earthquakes of size $M_w=5.0, 5.5, 6.0, 6.5, 7.0,$ and 7.5 as well as the 1992 event using stochastic finite fault technique as implemented in the computer program EXSIM [6]. For this purpose, the region of interest is defined as a rectangular box bounded by $39.45^\circ-39.54^\circ$ longitudes, $39.70^\circ-39.78^\circ$ latitudes. Then, to simulate horizontal components of full time series of ground motions, a total of 123 grid points are considered inside of this region. For simulation of all scenarios, the source, path, and site parameters are adopted from a previous study by Askan *et al.* [3].

Fig. 2 illustrates the spatial distribution of the simulated Peak Ground Acceleration (PGA) and Peak Ground Velocity (PGV) within the city center for the 1992 Erzincan earthquake ($M_w=6.6$) as a sample. It is noted that all of the generated earthquakes are baseline corrected and 4th order bandpass filtered at 0.25-25 Hz. The results of the predicted 1992 Erzincan earthquake yield that the city center experiences maximum PGA and PGV values of around $1g$ and 85 cm/s , respectively. As stated previously, Erzincan city center is placed on a deep alluvial basin in the close vicinity of the fault plane. It was recorded that, in spite of the moderate size of 1992 Erzincan earthquake, the residential structures suffered from significant levels of damage during the earthquake. Thus, these higher amplitudes of estimated seismic intensities are believed to explain the observed widespread fatalities.

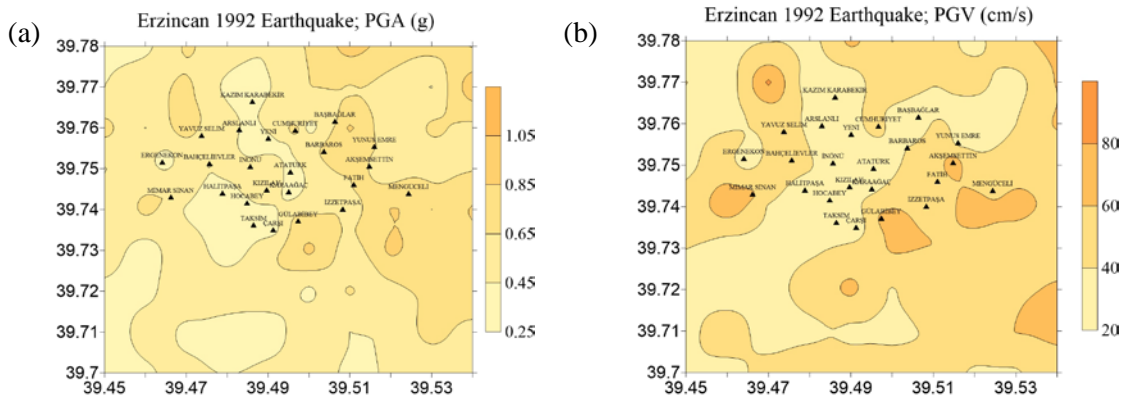


Fig. 2 – Spatial distribution of the simulated (a) PGA (b) PGV values of the 1992 Erzincan earthquake

4. Regional Building Stock

This section first presents the identification of building stock based on the observed data during field survey in the study region. The next part deals with idealization of the existing buildings with Equivalent Single Degree OF Freedom (ESDOF) models.

4.1 Identification of the regional buildings

Based on the results of a walk-down survey in the city center of Erzincan, all building stock is classified into 21 groups including 12 reinforced-concrete and 9 masonry subclasses. Among these subclasses, reinforced concrete structures are considered as either frame type, shear wall type (actually tunnel form) or dual type (i.e. frame with shear walls). Major structural parameters used in the classification of buildings are structure type, number of stories, and level of compliance with the seismic design and construction principles. In classification of all subclasses, the first two letters in the abbreviated names account for the type of structural system, where ‘RF’ stands for RC frame buildings, ‘RW’ for RC tunnel-form (shear wall system), ‘RH’ for RC dual-type (shear wall and frame), and ‘MU’ for unreinforced masonry subclasses. The number in the next digit shows the number of stories, where for masonry classes ‘1’, ‘2’, or ‘3’ indicates 1 story, 2 story, or 3 story, and for all three RC groups, ‘1’ or ‘2’ corresponds whether the building is low-rise (number of the story is between 1 and 3) or mid-rise (number of stories is between 4 and 8), respectively. The letter in the last digit ‘A’, ‘B’, or ‘C’ denotes the high, moderate, and low level of compliance with seismic design codes and construction principles. For example, RF2A represents earthquake-resistant mid-rise RC frame buildings whereas MU2C represents deficient (with many violations regarding earthquake resistant design and construction principles) 2 story masonry buildings.

4.2 Idealization of the regional buildings

In this study, for the sake of computational efficiency, buildings are idealized into ESDOF models by specifying three basic structural parameters; period (T), strength ratio (η), and ductility factor (μ). This simplified approach have been employed in earthquake engineering for a long time that goes back to the early work of Biggs [9], followed by many well-known studies [10-12]. The use of ESDOF models is considered to be reasonable since the study deals with a population of ordinary residential buildings instead of individual and particular buildings. In addition, from the field survey it is observed that the surveyed residential buildings are generally regular in plan and elevation with approximately homogeneous distribution of floor mass and stiffness, which are in favor of using ESDOF systems.

For seismic response evaluation of the ESDOF models Nonlinear Time History Analysis (NLTHA) in OpenSees platform [13] is performed. For this purpose, it is essential to select a robust hysteresis model which is capable of estimating the inelastic behavior of the real structural systems under earthquake excitations in a reasonably accurate way. In this study, to assess the effect of deterioration characteristics of structural systems on the final fragility curves, among different hysteresis models, the one proposed by Ibarra *et al.* [14], named as “Modified Ibarra –Medina-Krawinkler Deterioration Model”, is used. Ibarra *et al.* [14] verified that their



hysteresis peak-oriented deterioration model is able to estimate the inelastic dynamic response of reinforced-concrete structures during collapse with an acceptable degree of accuracy. The proposed deterioration model has then been used in different studies and for different structural types [e.g.: 15, 16] and the results of these studies seem to be promising.

To assess the ESDOF structural parameters, period, strength ratio, and ductility factor (T , η , and μ) are considered as random variables with mean and standard deviation values. The other hysteretic model parameters (α_s : post yield to elastic stiffness ratio, α_c : post-capping to elastic stiffness ratio, λ : residual strength to the yielding strength ratio, and γ : the hysteretic energy dissipation parameter) are taken constant with a single value. Table 1 lists ESDOF structural parameters for all sub-classes. The details of procedure for obtaining these parameters can be found in Karimzadeh [17].

Table 1 – Proposed ESDOF parameters for all building sub-classes

Frame ID	T (s)		η		μ		α_s (%)	α_c (%)	λ	γ
	Mean	St.D.	Mean	St.D.	Mean	St.D.				
RF1A	0.38	0.18	0.40	0.08	9.00	3.12	4	-20	0.20	800
RF1B			0.30	0.11	7.30	2.02	4	-25	0.20	400
RF1C			0.23	0.06	4.90	1.47	4	-30	0.20	200
RF2A	0.70	0.27	0.34	0.11	7.10	2.25	4	-20	0.20	800
RF2B			0.26	0.09	6.10	1.75	4	-25	0.20	400
RF2C			0.17	0.06	5.10	1.38	4	-30	0.20	200
RW1A	0.05	0.02	1.95	0.55	3.00	1.10	8	-20	0.20	1200
RW2A	0.15	0.05	1.30	0.36	2.70	0.90	8	-20	0.20	1200
RH1A	0.08	0.04	0.93	0.31	5.40	1.70	4	-20	0.20	1000
RH1B			0.77	0.25	4.50	1.40	4	-25	0.20	500
RH2A	0.43	0.18	0.59	0.17	4.90	1.40	4	-20	0.20	1000
RH2B			0.47	0.13	4.00	1.20	4	-25	0.20	500
MU1A	0.06	0.02	0.86	0.17	3.53	0.71	0	-20	0.20	600
MU1B			0.64	0.13	3.43	0.69	0	-25	0.20	300
MU1C			0.38	0.08	3.32	0.66	0	-30	0.20	150
MU2A	0.12	0.03	0.69	0.17	2.75	0.69	0	-20	0.20	600
MU2B			0.43	0.11	2.62	0.66	0	-25	0.20	300
MU2C			0.23	0.06	2.56	0.64	0	-30	0.20	150
MU3A	0.17	0.05	0.43	0.13	2.20	0.66	0	-20	0.20	600
MU3B			0.27	0.08	2.12	0.64	0	-25	0.20	300
MU3C			0.14	0.04	2.05	0.62	0	-30	0.20	150

5. Derivation of Fragility Curves

Fragility curve for a certain class of structural system is a continuous function describing the probability of exceeding a predefined damage level for specific levels of ground motion intensity. To derive fragility curves, three structural performance levels are considered: Immediate Occupancy (LS_1), Life Safety (LS_2), and Collapse Prevention (LS_3).

5.1 Fragility curve generation methodology

Fig. 3 is the schematic representation of the applied procedure for generation of fragility curve. Fig. 3-a shows distribution of a sample response statistics where the horizontal and vertical axes correspond to the ground motion intensity and the response parameter, respectively. The horizontal line labeled as LS_i presents the target limit state. The scattered data of the j^{th} ground motion intensity level (GMI_j) is selected in Fig. 3-b. The conditional probability of attainment or exceedance of the i^{th} limit state (LS_i) at the j^{th} ground motion intensity level is calculated as follows:

$$P[D \geq LS_i | GMI_j] = \frac{n_A}{n_T} \quad (2)$$

where, n_A is the sum of responses equal or above the i^{th} limit state, and n_T stands for the total number of responses at the j^{th} ground motion intensity level. After repeating these processes for different intensity levels, the discrete fragility information as presented in Fig. 3-c can be obtained for a certain limit state. A cumulative lognormal distribution function is fitted on the obtained data with least squares technique as illustrated in Fig. 3-d. To derive fragility curves for all subclasses, this process is repeated for all three limit states and 21 subclasses.

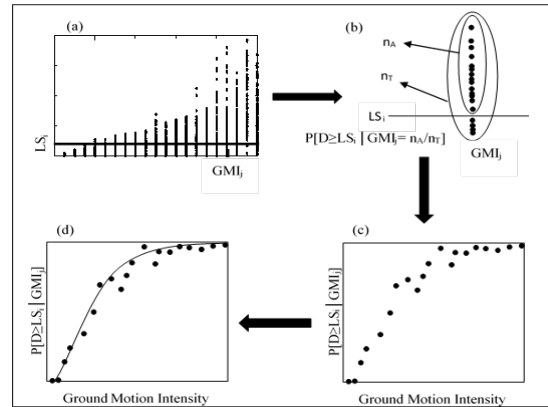


Fig. 3 – Schematic representation of the fragility curve generation procedure

5.2 Ground motion variability

In this study fragility curves are derived based on regional ground motion dataset since characteristics of the input ground motion records have large impact in the generated curves. Erzincan is a region with sparse ground motion networks, thus, to consider the regional effects, input ground motions are taken from the simulated ground motion dataset generated by the stochastic finite-fault methodology as described in Section 3.

The results from previous studies reveal that PGV and PGA correlate well with inelastic response of flexible structures (RC frame) and stiffer structures (masonry), respectively [18, 19]. Since the governing structural types in Erzincan include both RC and masonry buildings, to provide a strong correlation between hazard parameters and non-linear responses of the existing building sub-classes, ground motion records selected for fragility curve generation are separated into two groups: The first group is constituted according to PGV (for RC buildings) and the second group is formed with respect to PGA (for masonry buildings) as the intensity parameter. Overall, the selected simulated records cover a broad range of magnitudes between 5 and 7.5. The closest distance to the fault plane varies between 0.26-17.55 km. In order to have an even distribution for responses of the structures, each ground motion set, which is categorized according to PGV or PGA, is subdivided into 20 intensity levels by considering intervals of PGV=5 cm/s or PGA=0.05g, respectively.

To account for the variability in demand, for each ground motion set, a total of 200 records are selected such that for each intensity level there are 10 time histories with different soil conditions, distance and magnitude values.

5.3 Structural simulations and response statistics

In this paper, T , η , and μ parameters are considered as random variables. Lognormal distribution is assumed as the probability distribution function of the random variables since it results in positive values. Using Latin Hypercube Sampling method, for each of the random variables corresponding to the mean values of period, strength ratio, and ductility factor, 20 samples are generated. As a result, the sample size in each subclass is considered to be 20. The remaining model parameters including α_s , α_c , λ , and γ are assumed to be constant for all 20 simulated buildings from each subclass.

For a single subclass, since there exist 20 buildings, and the number of records in a specified intensity level (PGV or PGA) is 10, the number of response data points for an intensity level counts as 200. Since there are



totally 20 intensity groups, the number of SDOF analyses required to obtain the response statistics becomes 4000. NTHA is performed to reach the structural responses, which is assumed to be maximum ESDOF displacement.

5.4 Definition of limit states

In this study, constant limit states are considered to derive fragility curves [17]. The values are listed in Table 2

Table 2. Limit states in terms of displacement for all sub-classes

Frame ID	LS1 (cm)	LS2 (cm)	LS3 (cm)
RF1A	1.55	6.70	12.40
RF1B	1.40	6.30	11.60
RF1C	1.32	5.80	10.70
RF2A	2.40	8.55	16.10
RF2B	2.00	8.10	15.20
RF2C	1.65	7.11	14.30
RW1A	0.40	1.00	3.30
RW2A	0.80	1.90	4.50
RH1A	0.40	1.80	5.50
RH1B	0.28	1.40	3.10
RH2A	1.60	5.90	9.50
RH2B	1.20	4.80	8.80
MU1A	0.07	0.25	1.54
MU1B	0.05	0.18	1.13
MU1C	0.03	0.10	0.87
MU2A	0.23	0.63	2.08
MU2B	0.14	0.37	1.67
MU2C	0.08	0.29	1.45
MU3A	0.32	0.954	3.125
MU3B	0.20	0.63	2.50
MU3C	0.11	0.52	1.88

5.5 Building Specific Fragility Curves

Fig. 4 and Fig. 5 show the final smooth fragility curves. Comparison of the results show that for a given ground motion level, as the number of stories increases, the potential of damage increases for all building types. Also, in all cases, as the level of compliance with seismic design and construction codes gets worse, the probability of exceeding the ultimate limit state (LS_3) increases. For immediate occupancy limit state (LS_1), regardless of the level of compliance of structures with seismic design codes, the results of subclasses with the same number of stories and structural system are close to each other. However, for life safety (LS_2) and especially for collapse prevention limit states, the results deviate from each other. If the curves are compared with respect to the building types considered, it is observed that among RC buildings, RW sub-classes have the best seismic performance followed by RH sub-classes (Fig. 4). On the other hand, the RF buildings seem to exhibit different levels of performance depending on the specific characteristics of each sub-class. Finally, masonry sub-classes seem to exhibit a wide range of seismic response just like the RC frame buildings since they are generally non-engineered structures without any standards regarding the material quality and the construction technique (Fig. 5). Above observations show that the fragility curve sets of building sub-classes can simulate the inherent characteristics of the buildings in the study region in justifiable terms. Then, the use of this fragility information for seismic damage estimation in Erzincan is validated.

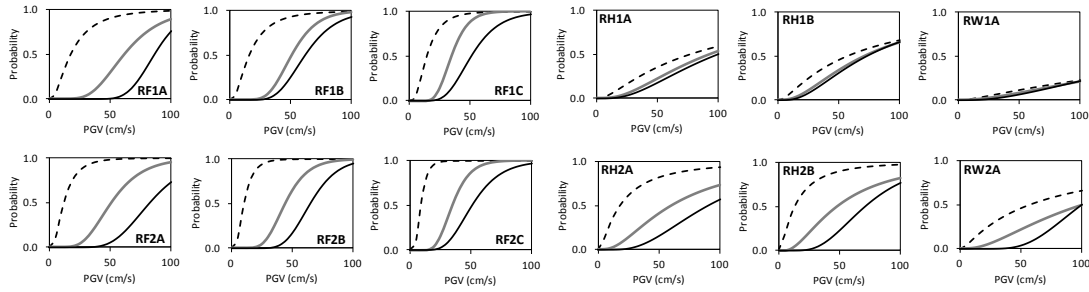


Fig. 4 – Fragility curves for RC subclasses using the first group of records categorized based on PGV where the dashed lines correspond to LS1, the gray solid lines to LS2, and the black solid lines to LS3

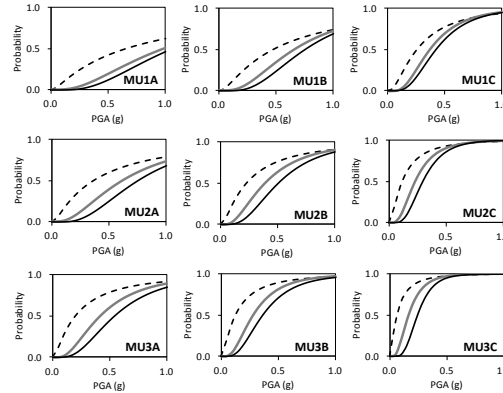


Fig. 5 – Fragility curves for masonry subclasses using the second group of records categorized based on PGA where the dashed lines correspond to LS1, the gray solid lines to LS2, and the black solid lines to LS3

6. Seismic Damage Estimation in Erzincan using Regional Ground Motions and Local Building Data

This section includes the methodology for seismic damage estimation and a verification exercise where the estimated damage for the 1992 Erzincan earthquake is compared against the observed one. Next, the potential seismic damage for a scenario event of $M_w=7$ is presented as a sample for prediction of potential losses.

6.1 Seismic damage estimation methodology

To estimate distribution of seismic damage in the study area, in the present study, Mean Damage Ratio (MDR) which expresses the disaggregated damage estimates with a single value as implemented by Askan and Yucemen [20] is chosen. For the computation of MDR, Damage Probability Matrix (DPM) is employed. Each column of DPM expresses a constant level of ground motion intensity, while each row of this matrix stands for a certain damage state. So, each element of this matrix, denoted as $P(DS, I)$, shows the probability of experiencing a certain damage state (DS) when the structure under consideration is subjected to a specified ground motion with intensity level of I:

$$P_k(DS, I) = \frac{N(DS, I)}{N(I)} \quad (3)$$

where, $N(I)$ is the number of k^{th} -type of buildings in the area subjected to a ground motion of intensity I and $N(DS, I)$ is the number of structures in damage state (DS), among the $N(I)$ buildings. To express the damage ratios in a more comparable way, the discrete values corresponding to each intensity level are converted to a single value as MDR. MDR is expressed as follows:

$$MDR(I) = \sum_{DS} P_k(DS, I) \cdot CDR(DS) \quad (4)$$



where, CDR(DS) is the central damage ratio corresponding to damage state DS. In this study, since a certain fragility curve set corresponding to a specified building class are derived for three limit states, the constructed DPM has 4 damage states as none (DS1), light (DS2), moderate (DS3), and severe (DS4). It is noted that, for all damage states the values corresponding to the CDRs are taken from Gürpınar *et al.* [21] which are proposed for Turkey.

6.2 Assessment of seismic damage in Erzincan

For seismic damage estimation, a total of 16 residential districts in Erzincan city with available building data are selected. Then, simulated records at the 16 residential areas for the 1992 Erzincan earthquake ($M_w=6.6$) and scenario event with $M_w=7$ are gathered. Since fragility curves of RC and masonry buildings are derived in terms of PGV and PGA, respectively; PGA and PGV values corresponding to center of each considered district are obtained from the simulated records. For the selected residential districts, percent distribution of the buildings with respect to the structural type as well as number of stories is achieved. Using the derived fragility curves, DPMs for all building types in each district under the given ground motion value are developed. Finally, through percent distribution of buildings in the selected locations, a single MDR is calculated for each residential area.

Spatial distribution of the estimated PGA as well as PGV for the 1992 Erzincan scenario earthquake ($M_w=6.6$) in the district centers is presented in Fig. 6. Similarly, the spatial distribution of the estimated PGA and PGV for the scenario event with $M_w=7$ in the selected district centers is illustrated in Fig. 7. Fig. 8 and Fig. 9 present spatial distribution of the buildings with respect to structural system and number of stories at the district centers collected as a walk-down survey. Fig. 10-a illustrates distribution of the observed MDRs for the selected residential districts where N/A Data corresponds to the geounits in which observed damage levels during the 1992 Erzincan earthquake are not available. Fig. 10-b presents distribution of the estimated MDRs for the selected residential areas where N/A Data corresponds to the residential districts in which the building information is not available. Comparison of the observed and estimated damage levels for the 1992 Erzincan earthquake demonstrates that for almost 75% of the residential districts the results are consistent. For the other geounits, the estimated damage levels are slightly larger than the observed values. These discrepancies may be attributed to the subjectivity in assigning damage states for the buildings in the field. When the spatial distribution of buildings as well as ground motion intensity parameters in terms of either PGA or PGV is compared with the spatial distribution of the estimated MDRs for the 1992 Erzincan earthquake, it is observed that all of them are in agreement. For instance, districts such as Fatih, İzzetpaşa, Akşemsettin, Cumhuriyet, Barbaros including mostly unreinforced masonry structures along with highest levels of PGA, have larger MDRs (in between 30%-50%) compared to the other districts. In contrast, for districts such as Atatürk and Halitpaşa, the estimated PGA values are lower in spite of existence of higher percentage of masonry buildings. As a result, the estimated MDRs are in between 10%-30%, less than the previously mentioned districts. At district Yavuz selim, although most of the buildings are newly constructed RC types, larger values of PGV result in larger MDRs (30%-50%). The minimum estimated MDR corresponds to Ergenekon (1%-10%). This is logical since Ergenekon has highest percentage of RC structures along with lowest PGV value.

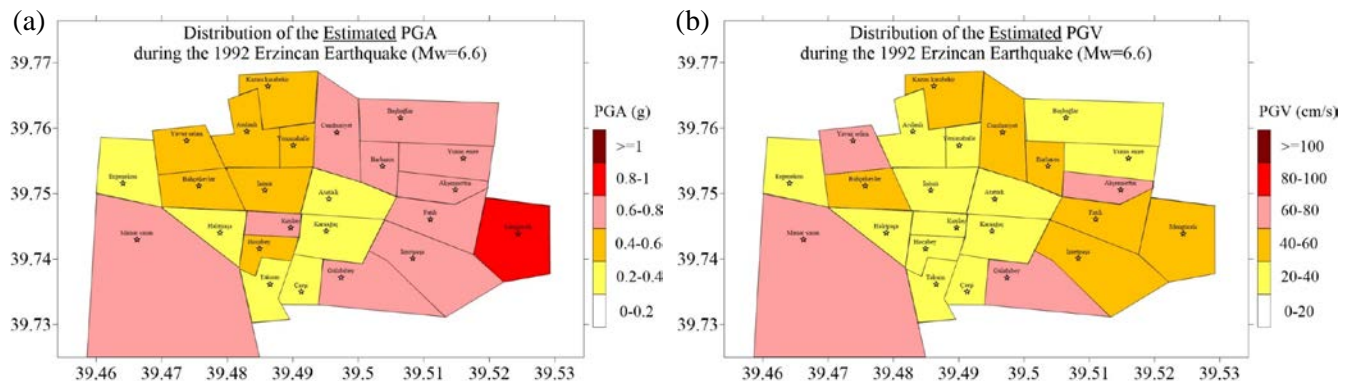


Fig. 6 – Spatial distribution of the simulated (a) PGA (b) PGV values of the 1992 Erzincan earthquake in the districts (Erzincan)

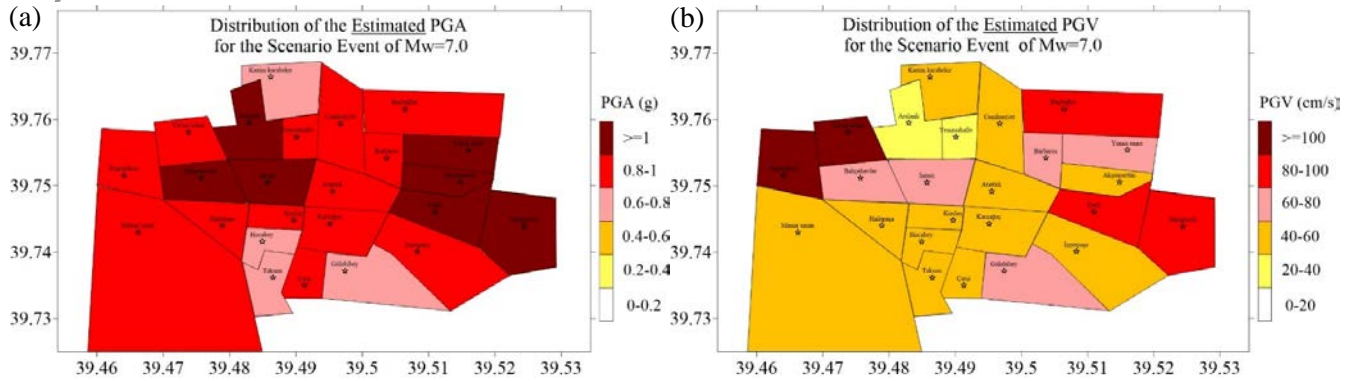


Fig. 7 – Spatial distribution of the estimated (a) PGA (b) PGV for scenario event of Mw=7.0 in the districts (Erzincan)

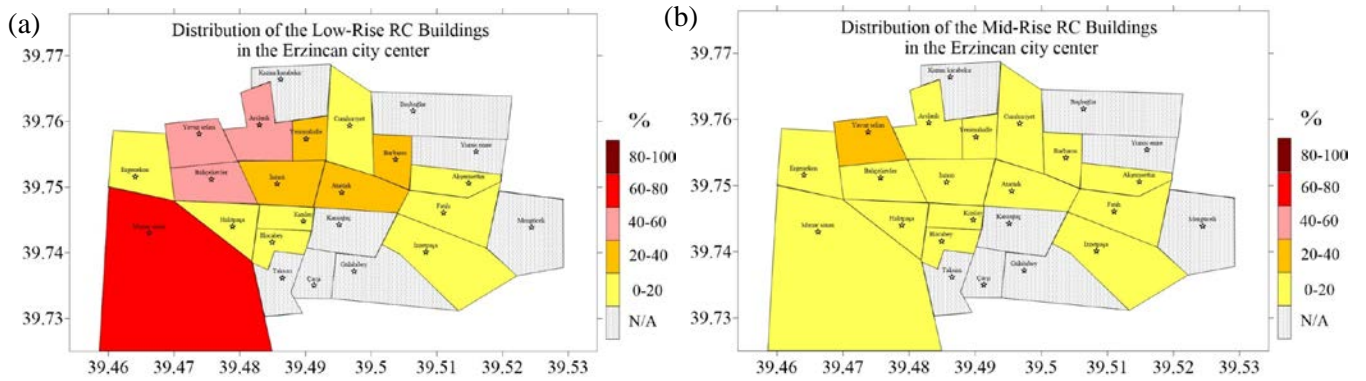


Fig. 8 – Spatial distribution of the (a) low-rise (b) mid-rise RC buildings in the districts (Erzincan)

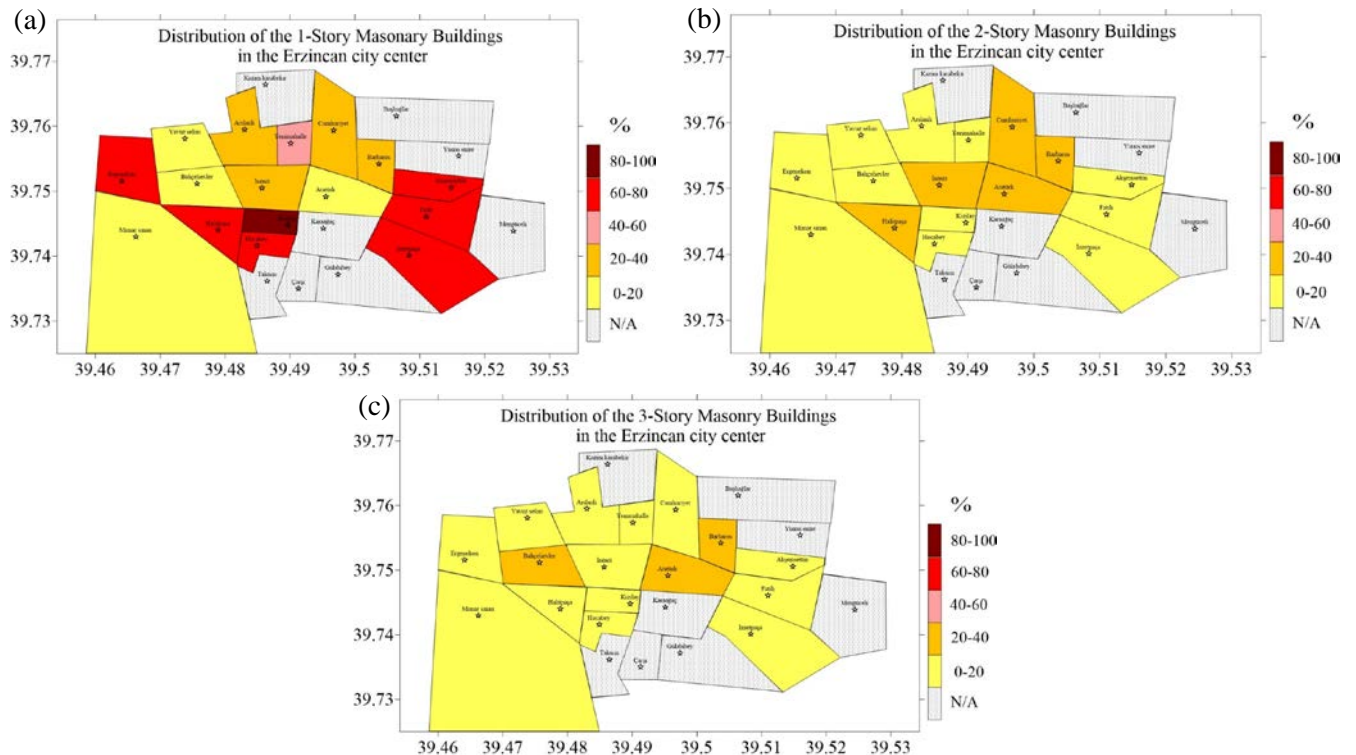


Fig. 9 – Spatial distribution of the (a) 1-story (b) 2-story (c) 3-story masonry buildings in the districts (Erzincan)

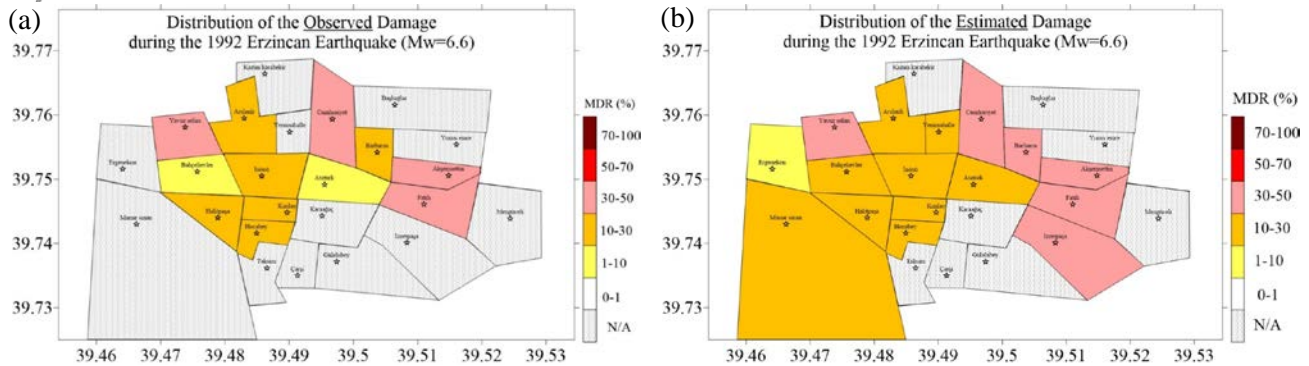


Fig. 10 – Spatial distribution of the (a) observed and (b) estimated MDRs in the Erzincan region for the 1992 Erzincan earthquake

After validating the method for the 1992 earthquake, distribution of the potential seismic damage for the scenario event of Mw=7 is anticipated and showed in Fig. 11. The damage estimates for the scenario event of Mw=7 reveal that six of the residential areas experience severe damage (50% \leq MDR \leq 100%). However, the estimated damage in the rest of the residential areas are moderate (10% \leq MDR \leq 50%). Therefore, for scenario event of Mw=7, the estimated damage levels show that the Erzincan city center is subjected to the moderate to heavy damage levels which is consistent with the regional seismicity and the structural vulnerability.

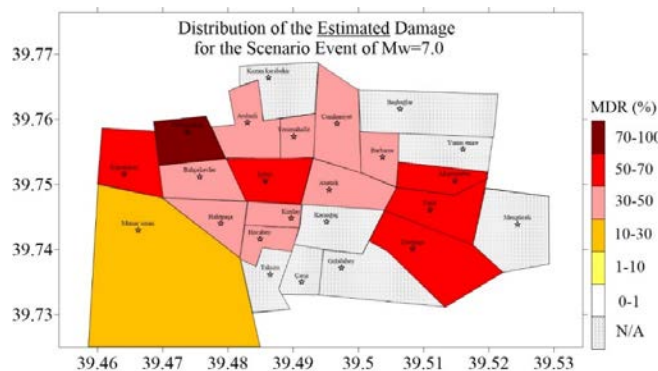


Fig. 11 – Spatial distribution of the estimated MDR in the Erzincan region for scenario event of Mw=7.0

7. Conclusions

In this study, seismic damage estimation of Erzincan is performed considering both regional seismic hazard and local building data. For this purpose, stochastic finite-fault methodology is applied to generate simulated time histories compatible with regional seismicity and a comprehensive building database corresponding to the study area is assembled. Structural damage is estimated for 16 residential districts in the study area for the 1992 earthquake and a scenario event with Mw=7.0. Similar to the other seismic loss assessment methodologies, the methodology presented herein contain inherent uncertainties arising from various sources such as modeling errors involved with the ground motion simulation technique, assumption of input parameters, building data, fragility and damage estimation methodology. In spite of these uncertainties, based on the results of this study, a reasonable match between the observations and computed results for the 1992 Erzincan earthquake is obtained. This result points out that the existing uncertainties are negligible. Also, the significance of considering the specific characteristics of the earthquake rupture through ground motion simulations as well as local building information in the predicted damage estimates is shown. The estimated damage levels for a scenario event of Mw=7.0 in the city center reveal that Erzincan is under significant seismic threat due to its close distance from the fault system in the North, soft soil conditions within Erzincan basin as well as the seismic vulnerability of the building stock in the respective area. Thus, to mitigate potential future earthquake losses in the region, the built environment must be evaluated for seismic safety in detail.



8. References

- [1] Ugurhan B, Askan A, Erberik MA (2011): A methodology for seismic loss estimation in urban regions based on ground-motion simulations. *Bulletin of the Seismological Society of America*, **101** (2): 710–725.
- [2] Sørensen MB, Lang DH (2014): Incorporating simulated ground motion in seismic risk assessment-application to the Lower Indian Himalayas. *Earthquake Spectra*, **31** (1), 71-95.
- [3] Askan A, Sisman FN, Ugurhan B (2013): Stochastic strong ground motion simulations in sparsely monitored regions: A validation and sensitivity study on the 13 March 1992 Erzincan (Turkey) earthquake. *Soil Dynamics and Earthquake Engineering*, **55**, 170-181.
- [4] Olsen KB, Archuleta RJ, Matarese JR (1996): Three-dimensional simulation of a magnitude 7.75 earthquake on the San Andreas fault. *Science*, **270** (5242), 1628.
- [5] Boore DM (1983): Stochastic simulation of high-frequency ground motions based on seismological models of the radiated spectra. *Bulletin of Seismological Society of America*, **73** (6A), 1865–1894.
- [6] Motazedian D, Atkinson GM (2005): Stochastic finite-fault modeling based on a dynamic corner frequency. *Bulletin of Seismological Society of America*, **95** (3), 995–1010. DOI:
- [7] Ugurhan B, Askan A (2010): Stochastic strong ground motion simulation of the 12 November 1999 Düzce (Turkey) earthquake using a dynamic corner frequency approach. *Bulletin of Seismological Society of America*, **100** (4), 1498-1512.
- [8] Mai PM, Imperatori W, Olsen KB (2010): Hybrid broadband ground-motion simulations: Combining long-period deterministic synthetics with high-frequency multiple S-to-S back-scattering. *Bulletin of Seismological Society of America*, **100** (5A), 2124-2142.
- [9] Biggs JM (1964): *Introduction to Structural Dynamics*. McGraw Hill Company, New York, 3.
- [10] Saiidi M, Sozen MA (1981): Simple Nonlinear Seismic Analysis of R/C Structures. *Journal of Structural Division*, **107** (5), 937–953.
- [11] Fajfar P, Fischinger M (1988): N2 - A Method for Non-Linear Seismic Analysis of Regular Structures. *Proceedings of the 9th World Conference on Earthquake Engineering*, 5, 111-116.
- [12] Qi X, Moehle JP (1991): Displacement Design Approach for Reinforced Concrete Structures Subjected to Earthquakes, *Earthquake Engineering Research Center (College of Engineering/University of California)*, **91** (2).
- [13] OpenSees 2.4.5. Computer Software, University of California, Berkeley, CA. Retrieved from <http://opensees.berkeley.edu>.
- [14] Ibarra LF, Medina RA, Krawinkler H (2005): Hysteretic models that incorporate strength and stiffness deterioration. *Earthquake Engineering and Structural Dynamics*, **34** (12), 1489–1511.
- [15] Ibarra LF, Krawinkler H (2005): Global collapse of frame structures under seismic excitations. *Rep. No. TB 152*, The John A. Blume Earthquake Engineering Center, Stanford University, Stanford, CA.
- [16] Lignos DG, Krawinkler H (2010): Deterioration modeling of steel components in support of collapse prediction of steel moment frames under earthquake loading. *Journal of Structural Engineering*, **137** (11), 1291-1302.
- [17] Karimzadeh Naghshineh S (2016): Use of simulated strong ground motion records in earthquake engineering applications, *Ph.D. Thesis*, Department of Civil Engineering, METU University, Ankara city, Turkey.
- [18] Erberik MA (2008-a): Generation of fragility curves for Turkish masonry buildings considering in-plane failure modes. *Earthquake Engineering and Structural Dynamics*, **37**(3), 387-405.
- [19] Erberik MA (2008-b): Fragility-based assessment of typical mid-rise and low-rise RC buildings in Turkey. *Engineering Structures*, **30** (5), 1360-1374.
- [20] Askan A, Yucemen MS (2010): Probabilistic methods for the estimation of potential seismic damage: Application to reinforced concrete buildings in Turkey. *Structural Safety*, **32** (4), 262-271.
- [21] Gürpınar A, Abalı M, Yüçemen MS, Yesilçay Y (1978): Feasibility of Obligatory Earthquake Insurance in Turkey. *Earthquake Engineering Research Center, Civil Engineering Department, Middle East Technical University, Ankara* (in Turkish), 78-05.